Mechanism of Flavin Mononucleotide Cofactor Binding to the *Desulfovibrio vulgaris* Flavodoxin. 1. Kinetic Evidence for Cooperative Effects Associated with the Binding of Inorganic Phosphate and the 5′-Phosphate Moiety of the Cofactor†

Tracey Arnold Murray and Richard P. Swenson*

Department of Biochemistry and Ohio State Biochemistry Program, The Ohio State University, Columbus, Ohio 43210

Received October 8, 2002; Revised Manuscript Received December 18, 2002

ABSTRACT: The pathway(s) by which the flavin cofactor binds to the apoflavoprotein is the subject of some debate. The crystal and NMR structures of several different flavodoxins have provided some insight, although there is disagreement about the location of the initial interaction between the flavin mononucleotide (FMN) and the apoflavodoxin and the degree of protein conformational change associated with cofactor binding [Genzor, C. G., Perales-Alcon, A., Sancho, J., and Romero, A. (1996) *Nat. Struct. Biol. 3*, 329−332; Steensma, E., and van Mierlo, C. P. M. (1998) *J. Mol. Biol. 282*, 653−666]. Binding kinetics using stopped-flow spectrofluorimetry and phosphate competition studies were used to develop a model for flavin binding to the flavodoxin from *Desulfovibrio vulgaris*. In the presence of phosphate, the time course of fluorescence quenching associated with FMN binding to apoflavodoxin was biphasic, whereas riboflavin, which lacks the 5′-phosphate group of FMN, displayed monophasic binding kinetics. When the concentration of phosphate in solution was increased, the FMN binding rates of the two phases behaved differently; the rate of one phase decreased, while the rate of the other increased. A similar increase in the single phase associated with riboflavin binding was also observed. This has led to the following model. The binding of the flavin isoalloxazine ring to its subsite is dependent on the presence of a phosphate group in the phosphate-binding subsite. When phosphate is in the buffer solution, FMN can bind in either of two ways: by the initial insertion of the 5′-phosphate group followed by ring binding or, when inorganic phosphate from solution is bound, the insertion of the isoalloxazine ring first. Riboflavin, which lacks the phosphate moiety of FMN, binds only in the presence of inorganic phosphate, presumably due to the binding of this group in the phosphate-binding subsite. These results suggest that cooperative interactions exist between the phosphate subsite and the ring-binding region in the *D. vulgaris* flavodoxin that are necessary for isoalloxazine ring binding.

The flavin cofactor−protein complex that constitutes the flavoprotein represents a remarkably versatile and efficient chemical partnership. Through the numerous enzymological and mechanistic studies that have been conducted over several decades, a good understanding of the catalytic or functional steps involving the cofactor has been established for many different flavoproteins. Structural studies have also yielded a great deal of detailed information about the many interactions between the flavin and the protein as well as the general environment provided by the protein. The molecular basis for the regulation of the redox properties and chemistry of the bound flavin through these interactions has been a focus of this and other laboratories. However, less is know about how the holoprotein complex is formed.

Flavodoxins are small, bacterial flavoproteins that participate in low-potential electron transfer pathways (*1*, *2*). Their small size, their well-established physical and structural properties, and the availability of highly expressing recombinant constructs make the flavodoxins good model systems for studying the properties and interactions of flavins and flavoproteins. All flavodoxins contain a single, noncovalently bound flavin mononucleotide (FMN)[1] cofactor. Cofactor binding occurs primarily through a combination of hydrogen bonds and aromatic interactions with the apoprotein. In the *Desulfovibrio vulgaris* flavodoxin, the FMN interacts with three loops of the protein: the teen's, 60's, and 90's loops. Two aromatic residues, Trp60 and Tyr98 from the 60's and 90's loops, respectively, flank either side of the FMN isoalloxazine ring (Figure 1) (*3*). The C2 and C4 carbonyl oxygen atoms as well as the N1, N3, and, in the reduced states, N5 of the ring are involved in hydrogen bonding with the protein backbone. Hydrogen bonding to ribityl side chain hydroxyls also contributes to cofactor binding. As in all flavodoxins, the 5′-phosphate moiety of FMN is bound in an atypical phosphate-binding site, anchored by several hydrogen bonds but with no ion pairing interactions (*3*).

The binding of flavins to flavodoxins has been studied since the late 1960s, most often using the flavodoxin from

† This study was supported in part by Grant GM36490 from the National Institutes of Health.

* To whom correspondence should be addressed: Department of Biochemistry, 776 Biological Sciences Bldg., The Ohio State University, 484 W. 12th Ave., Columbus, OH 43210-1292. Telephone: (614) 292-9428. Fax: (614) 292-6773. E-mail: swenson.1@osu.edu.

[1] Abbreviation: FMN, flavin mononucleotide.

10.1021/bi026967s CCC: $25.00
Published on Web 02/04/2003

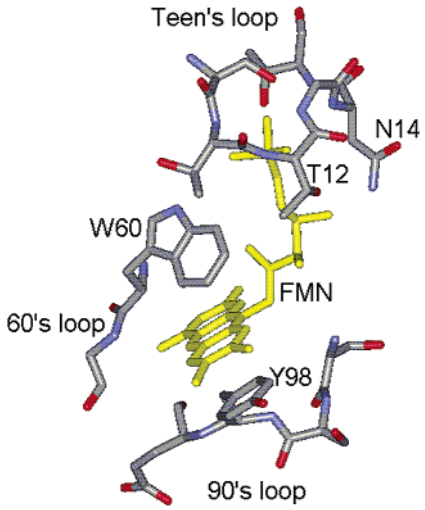

FIGURE 1: Depiction of the FMN-binding site in the *D. vulgaris* flavodoxin. This site is made up of three loops, designated the teen's loop, the 60's loop, and the 90's loop. The teen's loop makes hydrogen bonding contacts with the 5′-phosphate group and the ribityl side chain of the FMN. The 60's and 90's loops contribute the aromatic residues that flank either face of the isoalloxazine ring and also form hydrogen bonds with the heteroatoms in the pyrimidine ring.

Azotobacter vinelandii, also known as the Shethna flavoprotein. As early as 1968, Hinkson found that the binding of FMN to *A. vinelandii* flavodoxin occurred in a single kinetic phase as monitored by fluorescence quenching (*4*). This result was later confirmed for the *A. vinelandii* flavodoxin and others (*5*−*7*). However, Barman and Tollin found using the temperature-jump technique that the binding of FMN to the *A. vinelandii* and *Peptostreptococcus elsdenii* flavodoxins involves two relaxations, while only one relaxation is observed for riboflavin binding (*8*). This led to the proposal that the 5′-phosphate group of the FMN is required to induce a conformational change in the protein structure. They suggest that the initial binding of the phosphate group to the protein and the ensuing structural change allow for isoalloxazine ring binding. Other studies support the hypothesis that FMN binding involves some type of intermediate conformation and, thus, a more complicated binding mechanism, at least in the *A. vinelandii* flavodoxin (*9*, *10*). In contrast to the data for *A. vinelandii*, in experiments using a temperature jump to assess the binding of FMN to the *D. vulgaris* flavodoxin, only one phase of binding is observed (*11*). Also, stopped-flow binding studies conducted on three different flavodoxins (from *D. vulgaris*, *A. vinelandii*, and *Anabaena variabilis*) show monophasic fluorescence quenching for all with both FMN and riboflavin (*12*). These data led the authors to propose that the binding of either flavin to these flavodoxins was a simple second-order reaction.

The crystal structures of many of the flavodoxin holoproteins have been determined, *D. vulgaris* being one of the earliest to be determined (*3*, *13*). In 1996, Genzor et al. (*14*) published the first crystal structure of an apoflavodoxin, that from *Anabaena*. Its overall structure is similar to that of the holoprotein complex. However, the most striking difference is the "collapse" of residues into the flavin isoalloxazine ring-binding site. The tryptophan (Trp57) and tyrosine (Tyr94) which normally flank the *re* face and *si* face, respectively, of the isoalloxazine ring in this holoprotein are seen in the ring-binding site and are possibly making an alternative aromatic interaction with each other. This phenomenon has been described as the "closure of the tyrosine/tryptophan aromatic gate" (*14*). Also, the polypeptide loop containing the tryptophan adopts a different conformation in the apoflavodoxin structure. In contrast, the phosphate-binding loop is structurally well formed and appears to be occupied by either a sulfate or phosphate ion in an orientation similar to that of holoflavodoxin. The authors postulate that the initial site of the flavin−flavodoxin interaction is in this preformed phosphate site. However, subsequent NMR studies on the *A. vinelandii* apoflavodoxin indicate a greater flexibility of the entire flavin-binding region and the absence of a preformed phosphate-binding subsite (*15*). Because the X-ray structure was obtained from crystals grown in 3.2 M sulfate and 0.1 M phosphate, the authors of the NMR study suggest that the crystal structure could be a "freezing out" of one of the many possible conformations for the apoflavodoxin flavin-binding site and could not determine whether either the ring-binding subsite or the phosphate-binding subsite would be more favorable for initiating the flavin binding.

The study reported here was initiated to elucidate the mechanism of flavin cofactor binding to the flavodoxin from *D. vulgaris*. In this paper, we have examined the kinetic mechanisms of the binding of FMN and riboflavin to the wild-type *D. vulgaris* flavodoxin and mutants at the Trp60, Tyr98, Thr12, and Thr14 positions using stopped-flow spectrofluorimetry. In addition, the influence of inorganic phosphate on the kinetics of binding was evaluated. From these results, a minimal mechanism of flavin binding to flavodoxin is proposed. This model was further confirmed by near-UV circular dichroism, intrinsic fluorescence spectroscopy, and NMR analysis of the holoflavodoxin, the riboflavin−flavodoxin complex, and the apoflavodoxin (*16*).

EXPERIMENTAL PROCEDURES

Materials. The FMN used was either purchased from the Sigma-Aldrich Chemical Co. or extracted from recombinant wild-type flavodoxin from *Clostridium beijerinckii* and purified by anion-exchange chromatography. Riboflavin was purchased from General Biochemicals, Inc. All other chemicals were analytical reagent grade.

Site-Directed Mutagenesis, Protein Expression, and Purification. The Tyr98 mutants used in this study (Y98W, Y98F, Y98M, and Y98A) were prepared and characterized previously (*17*), as were the T12H and N14H mutants (*18*). The W60A mutation was introduced into the gene encoding the P2A or "pseudo wild type" *D. vulgaris* flavodoxin (*17*) by oligonucleotide-directed mutagenesis using the Kunkel method (*19*) and the 5′-GGAGTCGTCACCCGCGGTC-GAGCATCCG-3′ mismatched primer. The mismatched nucleotides are underlined. The first in that series represents a silent mutation that, along with the others, introduces a new *Sac*II restriction site that was used during the screening to the mutant plasmid. The nucleotide replacements and the sequence integrity of the entire coding region were confirmed by automated DNA sequence analysis. Protein expression and purification were carried out following established protocols (*17*, *18*). The expression levels of all of the mutants were comparable to that of the wild type, and all preparations used in these experiments were >95% pure on the basis of SDS−PAGE analysis.

Preparation of the Apoprotein and Determination of Apoprotein Extinction Coefficients. Apoflavodoxin was prepared using the standard trichloroacetic acid procedure (*18*, *20*) except that the 10% trichloroacetic acid solution was prepared in 0.1 M Tris-HCl (pH 8.0) instead of in 0.1 M potassium phosphate (pH 8.0) to ensure that no phosphate was present initially in the apoprotein preparations. The protein was then dialyzed overnight against the appropriate buffer. All experiments were performed with apoprotein prepared the previous day which had never been frozen.

The extinction coefficients at 278 nm of wild-type and mutant apoflavodoxins at 25 °C in 50 mM sodium phosphate buffer (pH 7.0) were established using the protocol of Pace et al. (*21*). The following values were obtained and used to determine the concentration of the apoflavodoxin solutions used in each experiment: 18 000 M^{-1} cm^{-1} for the wild type, 21 650 M^{-1} cm^{-1} for Y98W, 16 500 M^{-1} cm^{-1} for Y98F, 16 650 M^{-1} cm^{-1} for Y98A, 17 000 M^{-1} cm^{-1} for Y98M, and 12 800 M^{-1} cm^{-1} for W60A.

Stopped-Flow Kinetic Measurements. All of the kinetic experiments were performed on a Hi-Tech Scientific SF-61 stopped-flow spectrofluorimeter with an excitation wavelength of 446 nm and using a 530 nm cutoff filter in front of the orthogonal photomultiplier fluorescence detector. FMN extracted and purified from recombinant flavodoxin was used for all binding experiments. It is well-known that commercial preparations of FMN contain small amounts of flavin phosphorylated at positions other than the 5′-hydroxyl group of the ribityl side chain that can interfere with the binding of FMN. Indeed, kinetic time traces for fluorescence quenching contained an extra very slow phase (lasting several minutes) when commercial FMN was used. This phase was not present for the flavodoxin-derived FMN, which was therefore used exclusively throughout this study. The final concentration, after mixing, of FMN or riboflavin was constant and was always 1 μM. To achieve pseudo-first-order conditions, the final apoprotein concentration was 7.5, 10, 12.5, 15, or 17.5 μM. The rate constant at each apoprotein concentration was measured in triplicate. All experiments were conducted at 25 °C either in 50 mM sodium phosphate buffer (pH 7.0) or, for the phosphate competition experiments, in 38.3 mM Tris-HCl buffer containing from 0 to 150 mM sodium phosphate (pH 7.0). The ionic strength of these buffers was kept constant at 300 mM using appropriate concentrations of NaCl. The kinetic reactions were over in less than 30 s.

Determination of Dissociation Constants. The dissociation constants for the FMN complexes of the wild type as well as for the Y98W, Y98F, Y98A, T12H, N14H, and W60A mutants were measured fluorimetrically with a Jobin Yvon Horiba Fluoromax 3 spectrofluorimeter using established procedures (*22*). The dissociation constants for the riboflavin complex of the mutant proteins were measured spectrophotometrically using a Hewlett-Packard HP8452A diode array spectrophotometer as described previously (*22*). All dissociation constants were determined at 25 °C in 50 mM sodium phosphate buffer (pH 7.0). The concentrations of FMN and riboflavin were based on the published extinction coefficient at 446 nm of 12 500 M^{-1} cm^{-1} (*23*). In addition, the dissociation constants for the FMN and riboflavin complexes of wild-type flavodoxin were determined at 25 °C in 38.3 mM Tris-HCl buffer (pH 7.0) containing different concentrations of phosphate while keeping the ionic strength constant at 300 mM with the addition of NaCl as described above.

RESULTS

FMN and Riboflavin Binding to the Wild-Type and Tyr98 Mutant Flavodoxins. When flavin cofactors bind to apoflavodoxin, the intrinsic fluorescence of the isoalloxazine ring is almost completely quenched, providing a convenient way to follow the kinetics of binding by stopped-flow spectrofluorimetry (*5*). In contrast to earlier studies (*11*, *12*), FMN binding to the wild-type apoprotein was biphasic in our experiments, with the rate of both phases being concentration-dependent (Figures 2 and 3A). Similar biphasic reaction traces were observed for all of the Tyr98 mutants with FMN in 50 mM sodium phosphate buffer (pH 7.0) at 25 °C. Table 1 shows the second-order rate constants for the wild type and the Tyr98 mutants with both FMN and riboflavin. The wild-type, Y98F, and Y98W flavodoxins all had similar rates for both phases, whereas Y98A and Y98M exhibited much slower binding kinetics for both phases. The slower phase comprised approximately 80% of the overall amplitude of fluorescence quenching for the wild-type, Y98F, and Y98W proteins and more than 90% for the Y98A and Y98M flavodoxins. In contrast to FMN binding, the wild-type, Y98F, and Y98W apoproteins all bound riboflavin in a monophasic manner (Figure 3B). The rates were similar to the faster phase of FMN binding (Table 1). Interestingly, Y98A and Y98M did not measurably bind riboflavin in these kinetic experiments.

Dissociation Constants for the FMN and Riboflavin Complexes of the Tyr98 Mutant Flavodoxins. The K_d values for the FMN and riboflavin complexes of the wild-type flavodoxin from *D. vulgaris* have been measured previously (*18*, *24*), as has the K_d for the FMN complex of the Y98A mutant (*25*). [Because of its importance for comparisons to the mutants, we have repeated the determination of the K_d value for binding of FMN to the recombinant wild-type flavodoxin. We consistently obtain values that are 10-fold higher than the reported value (*24*). We use our value of 2.4 nM in our comparisons within.] The K_d values of the FMN complexes of Y98W and Y98F, as well as those for the riboflavin complexes of Y98W, Y98F, and Y98A, were also established in this study in 50 mM sodium phosphate (pH 7.0) at 25 °C (Table 1). None of the mutants bound the flavins as tightly as the wild type. The Y98W and Y98F mutants bound FMN 8- and 5-fold more weakly than the wild type, respectively, and bound riboflavin 3- and 4-fold more weakly, respectively. The Y98A flavodoxin did appear to bind to riboflavin in these experiments, but very weakly (data not shown), which made the accurate determination of the dissociation constant impossible using the method described here. On the basis of the limitations of this method, the K_d value for the riboflavin complex with Y98A was estimated to be greater than 0.5 mM.

Phosphate Effect on the Binding of FMN and Riboflavin to the Wild-Type Apoflavodoxin. From the crystal structures of the *Anabaena* apoflavodoxin (*14*) and the riboflavin complex of the *D. vulgaris* flavodoxin (*26*), a phosphate or sulfate ion appears to be able to bind to the phosphate-binding loop of the cofactor-binding site. Therefore, it seems

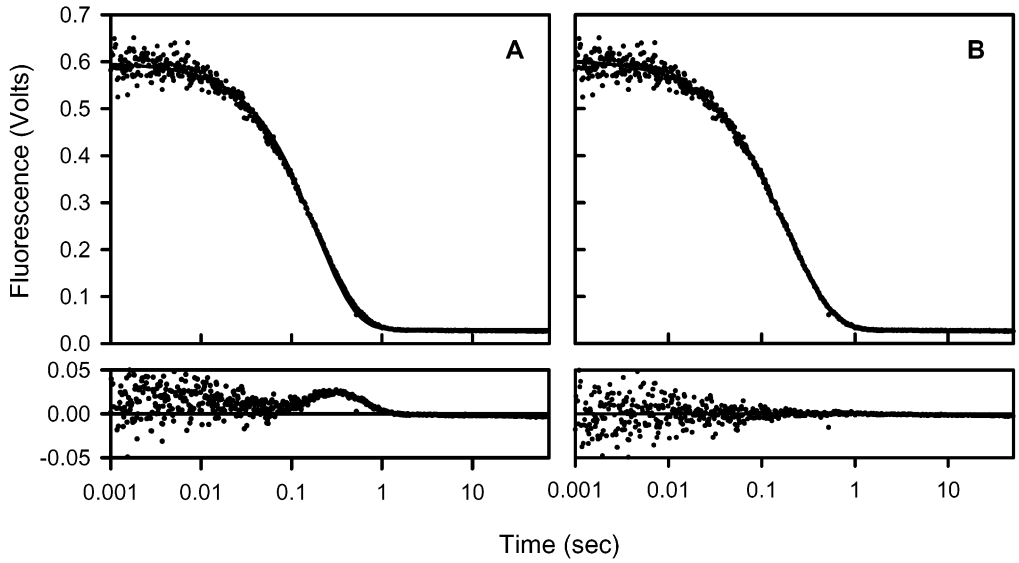

FIGURE 2: Stopped-flow kinetic traces of the fluorescence quenching associated with the binding of FMN to the wild-type apoflavodoxin from *D. vulgaris*. These experiments were performed by mixing an equal volume of 2 μM FMN with a solution containing an excess of apoflavodoxin, in this case, 15 μM, at 25 °C in 50 mM sodium phosphate (pH 7.0). The data are presented using a logarithmic time scale. (A) Fit of the experimental data to a single exponential. (B) Fit of the same data to two concurrent exponential reaction traces. The bottom window in each panel represents the "residuals" or differences between the experimental data and the theoretical fit in each case. Note that the fit involving two exponential curves (B) is significantly superior to the single-exponential fit.

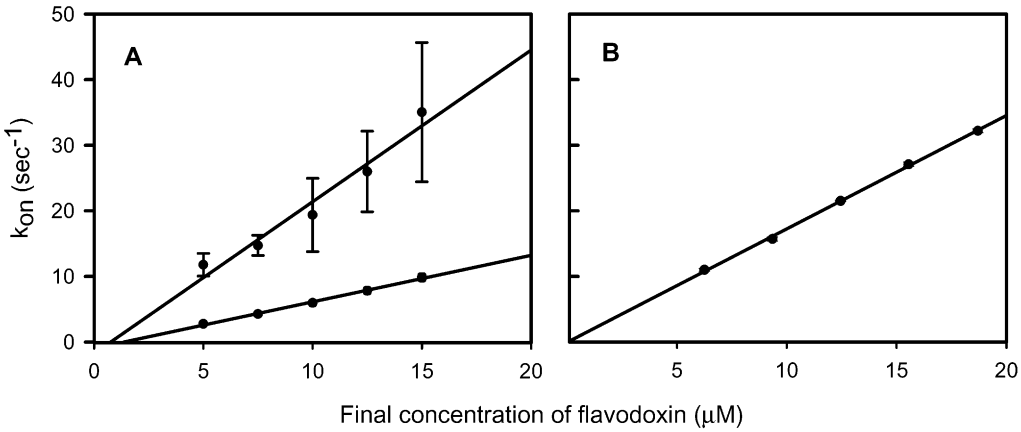

FIGURE 3: Plots of the observed rates of fluorescence quenching associated with each of the two kinetic phases of the binding of FMN (A) and the single kinetic phase of riboflavin binding (B) to wild-type *D. vulgaris* apoflavodoxin as a function of the final concentration of the apoprotein in 50 mM sodium phosphate (pH 7.0) at 25 °C. The final concentration of the flavin was 1 μM in each case. Data points are the average ± the standard deviation of triplicate stopped-flow kinetic experiments.

Table 1: Second-Order Rate Constants and Dissociation Constants[a] for Wild-Type and Y98 Mutant *D. vulgaris* Flavodoxin in 50 mM Sodium Phosphate Buffer (pH 7.0) at 25 °C

	FMN			riboflavin	
	slow phase (μM^{-1} s^{-1})	fast phase (μM^{-1} s^{-1})	K_d (nM)	rate (μM^{-1} s^{-1})	K_d (μM)
wild type	0.54 ± 0.03	1.8 ± 0.5	2.4 ± 0.7[b]	1.73 ± 0.02	0.51[c]
Y98W	0.356 ± 0.009	1.0 ± 0.2	19 ± 5	0.95 ± 0.02	1.3 ± 0.5
Y98F	0.255 ± 0.006	0.7 ± 0.2	13 ± 2	0.87 ± 0.01	2.1 ± 0.4
Y98M	0.045 ± 0.006	0.32 ± 0.06	ND	–	–
Y98A	0.0342 ± 0.0005	0.10 ± 0.08	3.2 ± 0.1[d]	–	–

[a] The second-order rate constants were determined by stopped-flow fluorimetry. The dissociation constants were determined by fluorescence spectroscopy for FMN and spectrophotometrically for riboflavin as described in Experimental Procedures. [b] From this work [this value is ca. 10-fold higher than that reported by Curley et al. (*24*)]. [c] From Zhou and Swenson (*18*). [d] From Zhou and Swenson (*25*).

reasonable that inorganic phosphate could compete with the 5′-phosphate of the FMN during its binding with the apoflavodoxin. To test this hypothesis, the rates of cofactor binding as monitored by stopped-flow fluorescence quenching were also measured in Tris-HCl buffer (pH 7.0) containing various concentrations of phosphate. Because flavin binding is dependent on ionic strength (*5*−*7*, *12*, *27*), the ionic strength was kept constant in these experiments using sodium chloride. Table 2 shows the results of these studies. With no phosphate present in solution, wild-type flavodoxin exhibited monophasic binding kinetics with FMN and did not bind riboflavin measurably at the concentrations used in

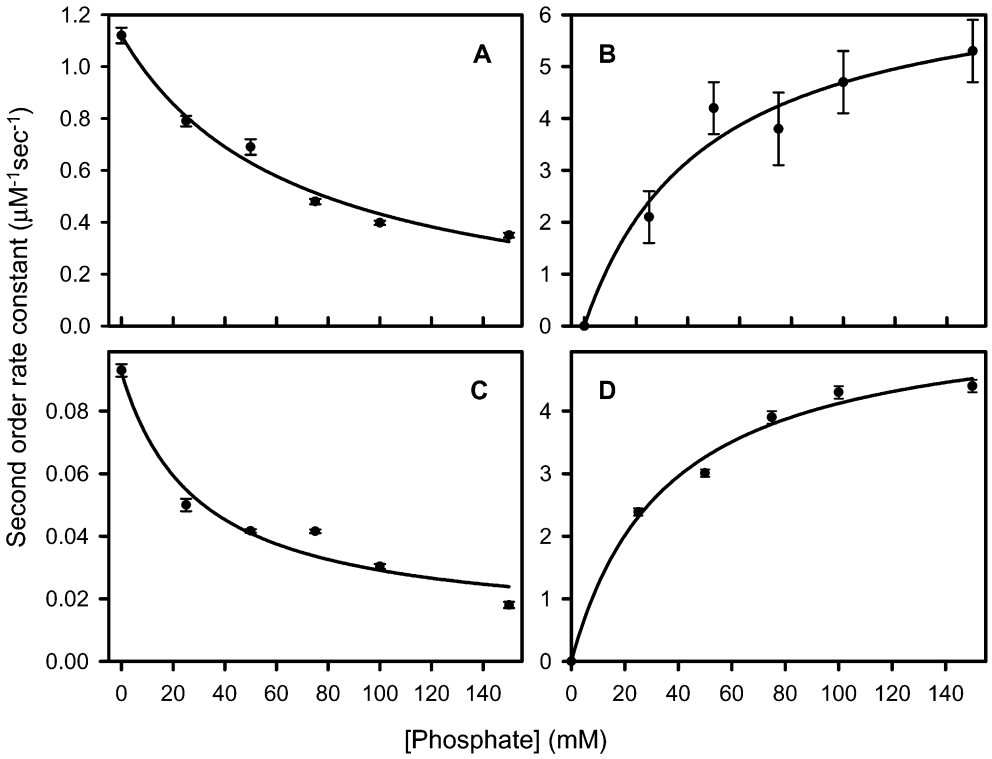

FIGURE 4: Effect of inorganic phosphate on the second-order rate constants for the binding of FMN to wild-type apoflavodoxin [slow phase (A) and fast phase (B)], FMN to the Y98A apoflavodoxin (C), and riboflavin to wild-type apoflavodoxin (D) at 25 °C and pH 7.0. The phosphate buffers and other reaction conditions are described in Experimental Procedures. The solid lines represent nonlinear regression fits of the data to a single-site binding isotherm. The average apparent dissociation constant obtained from these fits was 45 ± 9 mM.

Table 2: Second-Order Rate Constants[a] and Apparent Dissociation Constants[b] from the Phosphate Competition Studies[c] of Wild-Type and Y98A *D. vulgaris* Flavodoxins

	FMN and wild type		FMN and Y98A	riboflavin and wild type
[P_i] (mM)	slow phase (μM^{-1} s^{-1})	fast phase (μM^{-1} s^{-1})	rate (μM^{-1} s^{-1})	rate (μM^{-1} s^{-1})
0	1.1 ± 0.03	–	0.093 ± 0.002	–
25	0.79 ± 0.02	2.1 ± 0.5	0.050 ± 0.002	2.4 ± 0.06
50	0.69 ± 0.03	4.2 ± 0.5	0.042 ± 0.0006	3.0 ± 0.06
75	0.48 ± 0.01	3.8 ± 0.7	0.042 ± 0.0006	3.9 ± 0.1
100	0.40 ± 0.008	4.7 ± 0.6	0.030 ± 0.0008	4.3 ± 0.1
150	0.35 ± 0.009	5.3 ± 0.6	0.018 ± 0.001	4.4 ± 0.1
K_{app} (mM)	67 ± 24	47 ± 18	30 ± 15	36 ± 7

[a] The second-order rate constants were determined by stopped-flow fluorimetry. [b] The apparent dissociation constants were determined by plotting the second-order rate constants vs the concentration of phosphate and fitting to a binding isotherm. [c] Values are at pH 7.0, 25 °C, and an ionic strength of 300 mM in buffers described in Experimental Procedures.

the kinetic experiments. In the presence of phosphate, the binding of FMN again became biphasic, with approximately 80% of the amplitude associated with the slower phase and 20% with the faster phase at all phosphate concentrations. As the phosphate concentration was increased to 150 mM, the rate of the slower phase decreased and the rate of the faster phase increased. The rate of the single phase observed for the binding of riboflavin to the wild-type apoprotein also increased as the phosphate concentration was increased. The time courses for the fluorescence quenching associated with the binding of FMN to the Y98A apoflavodoxin were monophasic at all phosphate concentrations at this higher ionic strength (300 vs 88 mM previously), and the rates decreased with increasing phosphate concentrations. For the binding of FMN to the wild type and Y98A, as well as for the binding of riboflavin to the wild type, plots of the second-order rate constants as a function of the phosphate concentration all generated what appeared to be hyperbolic curves consistent with a phosphate binding isotherm (Figure 4). An average value for the apparent K_d for phosphate of 45 ± 9 mM was obtained from these analyses. These data suggest that both the inhibition and the enhancement of the rates are caused by the same phenomenon, the binding of inorganic phosphate to apoflavodoxin.

Because of this "phosphate effect" on the binding kinetics, the dissociation constants for both the FMN and riboflavin complexes of the wild-type *D. vulgaris* flavodoxin were evaluated. Previous binding studies for the wild-type *Anabaena* flavodoxin show no effect of phosphate on the K_d for riboflavin; however, the K_d for FMN decreases from 0 to 10 mM phosphate and then increases again with 100 mM phosphate (*28*). In our experiments with the *D. vulgaris* flavodoxin, phosphate had a stabilizing effect on both the FMN and riboflavin complexes (Table 3). This result is similar to that reported by Pueyo et al. (*12*) with *D. vulgaris* flavodoxin, although those experiments are not controlled for ionic strength. Again, the ionic strength of our buffers was carefully controlled with NaCl to make sure that the effect that was seen was due to the presence of phosphate and not to changes in ionic strength. The effect on the binding of riboflavin was the most pronounced, with the K_d changing from 94 ± 17 μM with no phosphate present to 0.46 ± 0.09 μM in the presence of 150 mM phosphate. A 9-fold decrease in the dissociation constant of the complex occurred with the addition of just 1 mM phosphate, suggesting a highly

Table 3: Dissociation Constants for Wild-Type *D. vulgaris* Flavodoxin with FMN and Riboflavin at Various Concentrations of Sodium Phosphate[a]

$[P_i]$ (mM)	FMN (nM)	riboflavin (μM)
0	11 ± 6	94 ± 17
1	10 ± 9	10 ± 2
5	5 ± 3	2.5 ± 0.3
10	1.7 ± 0.7	1.9 ± 0.6
25	0.7 ± 0.3	0.8 ± 0.3
50	0.3 ± 0.3	0.7 ± 0.2
100	0.3 ± 0.1	0.42 ± 0.006
150	0.42 ± 0.04	0.46 ± 0.09

[a] All values were obtained at 25 °C, pH 7.0, and a constant ionic strength of 300 mM as described in Experimental Procedures.

cooperative effect. Phosphate also stabilized the FMN complex, though not to the extent seen with riboflavin. The K_d of FMN dropped from 11 ± 6 nM with no phosphate to 0.42 ± 0.04 nM with 150 mM phosphate. The destabilizing effect seen with *Anabaena* was not observed for the *D. vulgaris* flavodoxin.

Kinetics and K_d's of the Phosphate-Binding Subsite Mutants T12H and N14H. To further examine this phosphate effect, two phosphate-binding subsite mutants were studied: the T12H and N14H mutants. These mutants were prepared for other experiments that were designed to place a positive charge in the phosphate-binding site potentially without the complete disruption of hydrogen bonding (*18*). Because it was expected that the effect of these substitutions would be localized to the phosphate-binding subsite, it was anticipated that the rate of binding of FMN might be affected, but not that for riboflavin. The binding of FMN to these mutants remained in the nanomolar range, though weaker than that of the wild type, with 8- and 4-fold increases in the K_d observed for T12H and N14H, respectively (Table 4). Surprisingly, these mutants also affected the binding of riboflavin to approximately the same extent: 8- and 6-fold increases in the K_d for T12H and N14H, respectively. These substitutions also affected the rate of binding of both FMN and riboflavin (Table 4). Like for the wild type, FMN binding to both of the mutants was monophasic in the absence of phosphate, with a second-order rate constant similar to that of the wild type (T12H slightly faster and N14H slightly slower). In both, as the concentration of inorganic phosphate was increased, FMN binding was again biphasic with the majority of the quenching occurring at the slower rate. Again, the slower rate was inhibited by increasing the phosphate concentration, and the faster rate was enhanced. As with the wild type, riboflavin did not bind to these mutants in the absence of phosphate. Interestingly, the monophasic rate of riboflavin binding was enhanced as the phosphate concentration was increased. These results suggested that there was some interaction between the phosphate-binding subsite and the rest of the flavin-binding region. The magnitude of the phosphate effect, on either the inhibition or the enhancement, was not as great in these mutants as it was in the wild type.

Kinetics and K_d of the W60A Mutant. The W60A mutation removed the aromatic group on the inner, or *re*, face of the isoalloxazine ring. This mutant behaved in a manner different from that of wild-type flavodoxin and all of the other mutants discussed thus far (Table 4). Like for the others, FMN binding was biphasic, but the two phases had more equal amplitudes (60% for the slower phase and 40% for the faster phase). Unlike for the wild type, FMN binding remained biphasic when no inorganic phosphate was present in the buffer and both phases showed competition with phosphate. This suggested a different mechanism of binding for this mutant. The K_d of the FMN complex of the W60A mutant was 63 ± 35 nM. This is weaker than those of both the wild type (2.4 nM) and Y98A (3.2 nM) (*25*). This mutant did not bind riboflavin at any phosphate concentration.

DISCUSSION

The mechanism of noncovalent binding of flavin cofactors to flavodoxins and other flavoproteins is not well understood. Several studies on flavodoxins suggest that the binding is completed in one step, with the 5′-phosphate group of the FMN making the first contact with the apoprotein (*4*−*7*, *11*, *12*). However, as additional methods were utilized, it was thought that the mechanism of binding would prove to be more complex (*8*−*10*). The hypothesis that a phosphate-triggered conformational change is required for the binding of the flavin isoalloxazine ring has its roots in papers published in the early 1970s (*7*, *8*). Because some flavodoxins are able to bind to riboflavin while others are not, researchers have hypothesized that the phosphate moiety is required for the binding of the isoalloxazine ring in the flavodoxins that cannot bind riboflavin. They postulate that, in these cases, the ring-binding subsite is closed and that phosphate is

Table 4: Second-Order Rate Constants for FMN and Riboflavin Binding and Apparent Dissociation Constants for the FMN and Riboflavin Complexes of the T12H, N14H, and W60A Mutants of the *D. vulgaris* Flavodoxins[a]

	T12H			N14H			W60A	
	FMN		riboflavin	FMN		riboflavin	FMN	
$[P_i]$ (mM)	slow phase (μM^{-1} s^{-1})	fast phase (μM^{-1} s^{-1})	rate (μM^{-1} s^{-1})	slow phase (μM^{-1} s^{-1})	fast phase (μM^{-1} s^{-1})	rate (μM^{-1} s^{-1})	slow phase (μM^{-1} s^{-1})	fast phase (μM^{-1} s^{-1})
0	1.3 ± 0.09	−	−	0.72 ± 0.03	−	−	0.69 ± 0.02	1.3 ± 0.09
25	1.2 ± 0.05	1.9 ± 0.9	1.0 ± 0.04	0.59 ± 0.02	1.4 ± 0.7	0.74 ± 0.02	0.37 ± 0.06	0.6 ± 0.1
50	1.0 ± 0.05	2.6 ± 0.6	1.8 ± 0.09	0.58 ± 0.02	2.3 ± 0.6	1.2 ± 0.02	0.35 ± 0.02	0.6 ± 0.1
75	0.93 ± 0.03	3.0 ± 0.7	2.2 ± 0.09	0.51 ± 0.008	2.7 ± 0.5	1.7 ± 0.03	0.27 ± 0.02	0.6 ± 0.1
100	1.0 ± 0.02	4.0 ± 0.7	2.5 ± 0.06	0.56 ± 0.02	3.1 ± 0.6	1.7 ± 0.03	0.14 ± 0.02	0.21 ± 0.05
150	0.86 ± 0.04	4 ± 1	2.9 ± 0.09	0.41 ± 0.02	4.0 ± 1.0	2.4 ± 0.08	0.15 ± 0.005	0.31 ± 0.01
K_{app} (mM)	76 ± 81	52 ± 15	74 ± 7	150 ± 230	93 ± 17	110 ± 36	38 ± 21	22 ± 19
K_d FMN[b] (nM)	18 ± 5			9 ± 2			63 ± 35	
K_d Ribo[b] (μM)			4 ± 1			3.1 ± 0.3		

[a] All values were obtained at pH 7.0 and 25 °C in the phosphate competition buffers at an ionic strength of 300 mM as described in Experimental Procedures. [b] Values are at 25 °C in 50 mM sodium phosphate buffer (pH 7.0).

required to trigger the conformational change that opens the ring-binding site. They also note larger differences between the circular dichroism spectra of apo- and holoflavodoxins that cannot bind riboflavin when compared to the differences between those that can (*7*). This idea also gained support from a time-resolved fluorescence study which seemed to show a form of FMN that was bound to the flavodoxin, yet with its isoalloxazine ring able to behave like free FMN (*10*).

The appearance of the first crystal structure of an apoflavodoxin (from *Anabaena*) seems to support some of these hypotheses. Evident in that structure is the "collapse" of the *re* face tryptophan and, to a lesser extent, the *si* face tyrosine into the isoalloxazine-binding subsite (*14*). The polypeptide loop containing the tryptophan residue also adopts a different conformation. The presence of a phosphate ion, or more likely a sulfate ion given the high concentrations of sulfate present in the crystallization buffer, in the phosphate-binding subsite, led the authors to suggest that this site is preformed in the apoflavodoxin structure and that this would probably be the site of the initial interaction between the flavin and the flavodoxin, as earlier investigators thought. In contrast, the absence of NMR cross-peaks for regions within all three loops that comprise the majority of the flavin-binding site suggests that this region of the apoprotein may actually be disordered or at least more flexible in solution (*15*). This raises the possibility that the crystal structure may not be representative of the apoflavodoxin solution structure.

The results of this study, which utilized both the wild type and a number of FMN-binding site mutants for the *D. vulgaris* flavodoxin, support a more complex binding mechanism which involves a phosphate-induced conformational change that promotes ring binding. During the initial part of our study, we observed biphasic kinetics for the quenching of the flavin fluorescence during the binding of FMN to the wild-type apoprotein, an observation that contrasts with some previously published studies (*11*, *12*). It is not obvious why this difference exists except that the two kinetic phases are not very well separated under some conditions and that the extent of quenching associated with the fast phase is relatively small. Therefore, it might be possible to overlook this minor phase. However, the contrasting responses of the two phases to increasing phosphate concentrations, the absence of a second kinetic phase for riboflavin binding using the same apoprotein preparations and studied under conditions identical to those used for FMN binding, and the consistent reproducibility of the results suggested that this biphasic behavior was not a technical artifact. Furthermore, biphasic fluorescence quenching time courses were also observed for some of the mutants studied and therefore persisted from one protein preparation to another.

The data we have presented in this paper have led us to develop the following minimal mechanism for the binding of FMN and riboflavin to the flavodoxin from *D. vulgaris* (Scheme 1). In this model, FMN can bind to the flavodoxin in either of two ways, phosphate-first (as postulated by others) or ring-first. On the basis of the biphasic binding kinetics of the stopped-flow fluorescence quenching experiments, both binding modes are possible in solution, as long as there is inorganic phosphate present. The binding of riboflavin was monophasic and, because it lacks the 5′-phosphate group of FMN, can only bind via the ring-first mode. In the absence of phosphate, the binding of FMN was monophasic and riboflavin did not bind measurably in the kinetic experiments. This led us to conclude that phosphate was required for the ring-first binding mode to occur.

Scheme 1: Representation of the Mechanism for the Binding of FMN (or riboflavin along the top loop) to the Apoflavodoxin from *D. vulgaris*[a]

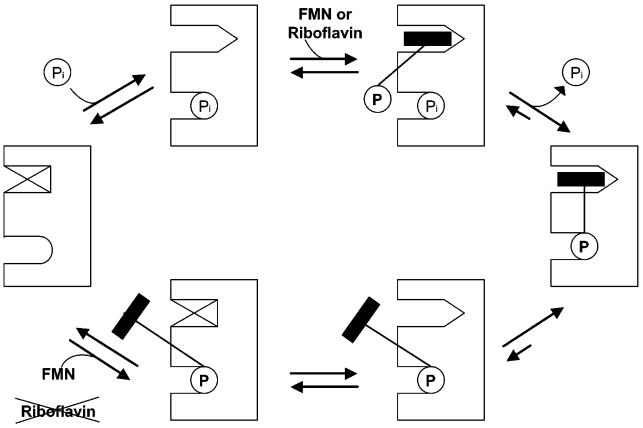

[a] P_i represents inorganic phosphate from the solution. The black rectangle represents the flavin isoalloxazine ring and the encircled P the 5-phosphate group. The top loop represents the ring-first binding mode that can occur when inorganic phosphate is bound. FMN and riboflavin can both bind via this mechanism. The bottom loop represents the phosphate-first binding mode in which the 5′-phosphate group of the FMN initially binds to the unoccupied phosphate-binding subsite; this mode is unavailable to riboflavin. In both mechanisms, the binding of a phosphate moiety triggers a change in the flavin-binding subsite that promotes ring binding.

The slower kinetic phase of FMN binding was assigned to the phosphate-first binding mode and the faster phase to the ring-first mode for the following reasons. In the presence of phosphate, the rate of fluorescence quenching associated with riboflavin binding was similar to the rate of the faster phase of FMN binding. Furthermore, this rate for riboflavin binding, like the faster phase for FMN, increased as the phosphate concentration increased. In contrast, the rate for the slower phase of FMN binding decreased. This would be predicted by the model; if the slower phase represented the phosphate-first binding mode, increasing inorganic phosphate levels should compete with the 5′-ribityl phosphate for the phosphate-binding subsite, decreasing the overall rate of FMN binding of this phase. In the absence of inorganic phosphate in the buffer solution, the fluorescence quenching associated with FMN binding was monophasic, presumably representing the maximal rate of the phosphate-first binding mode under these conditions. It is assumed that the ring-first binding mode does not exist under these conditions because of the lack of riboflavin binding. Finally, what is observed in the fluorescence quenching experiments is the binding of the isoalloxazine ring, not the binding of the phosphate moiety. Therefore, because the phosphate-first binding mode would require the interaction of the phosphate with the flavodoxin first, followed by isoalloxazine ring binding, this would appear as a rate of fluorescence quenching that was slower than that of the ring-first mode, which would result in quenching almost as soon as contact was made between the flavin and the apoflavodoxin.

This model is consistent with a phosphate-induced conformational change that promotes the ring-first binding mode. If the extent of fluorescence quenching is assumed to be

similar for each binding mode, the differences in amplitudes for the phases suggest that the majority of flavodoxin binds FMN via the slower, or phosphate-first, mode as most of the fluorescence quenching occurs at this rate. However, some of the flavodoxin is present in a form that is able to bind to the ring first. In the absence of phosphate, very little of the apoflavodoxin is in this ring-first conformation and the binding of FMN must go through the phosphate-first mechanism. As the phosphate concentration is increased, the rate of the faster phase increases in response to a greater amount of the ring-first competent protein present in solution. Except for the appearance of the second phase upon inclusion of inorganic phosphate in the buffer, the amplitudes of the two phases of fluorescence quenching did not correlate with increasing phosphate concentrations, but instead appeared to remain nearly constant throughout most of the concentration range. This suggests that the proposed binding model represents a minimal mechanism and that other steps may exist that we do not observe by fluorescence quenching.

The proposed model supports a phosphate-dependent binding event. Consistent with this conclusion, hyperbolic curves were obtained when the second-order rate constants for both phases of FMN binding and the single phase of riboflavin binding were plotted against the concentration of inorganic phosphate. The data could be fit to a single-site binding isotherm, generating apparent K_d values that were similar for both FMN and riboflavin (Figure 4 and Table 2). This suggested that all three of these interactions were caused by the same phenomenon. Because the concentration of phosphate in the buffer was the only variable, it seemed reasonable that these apparent K_d values must represent that of the inorganic phosphate−apoflavodoxin complex. An average apparent K_d for inorganic phosphate and apoflavodoxin of 45 ± 9 mM was obtained from all of the data. On the basis of this apparent K_d, at the concentrations of phosphate and/or sulfate used for crystallization of the apoprotein, this phosphate-binding site should be saturated. This is consistent with the extra density that was observed in the crystal structure in the phosphate-binding subsite of the FMN-binding site (*14*). All of these data together suggest that the phosphate kinetic effects reported here are the result of the binding of inorganic phosphate to the phosphate-binding subsite.

The data obtained from the mutants support this binding model. The phosphate-binding subsite mutants, T12H and N14H, were able to influence the binding of riboflavin, even though riboflavin has no 5′-phosphate moiety and therefore should be unaffected by mutations in this site. Phosphate effects were observed in both the rate constants and in the K_d of riboflavin with these mutants. When compared to that of the wild type, the K_d's of both the FMN and riboflavin complexes with either mutant are affected to the same extent (ca. 8-fold for FMN and 4−6-fold for riboflavin). Because riboflavin has no 5′-ribityl phosphate group, it could be assumed that these mutants would have no effect on its binding. However, the kinetic data demonstrated that riboflavin binding is dependent on phosphate binding. Therefore, any variable that affects the binding of the 5′-phosphate group of FMN is also likely to influence the binding of the inorganic phosphate in the riboflavin complex and be reflected in the dissociation constant of riboflavin. Just as for the wild type, both phases of the binding of FMN were also affected by increasing concentrations of inorganic phosphate; the slower (phosphate-first) phase was inhibited, while the faster (ring-first) phase was enhanced. Neither phase was affected to the extent seen in the wild type. This was expected for the phosphate-first phase because the mutations should have an effect on the binding of phosphate, and because these mutations also show an effect on the binding of riboflavin, the ring-first phase should be affected as well. Interestingly, when the second-order rate constants were plotted versus the concentration of phosphate in solution, an apparent K_d for phosphate very similar to that for wild-type apoprotein was obtained for the T12H mutant, whereas the N14H mutant generated a value twice as large. This suggested that the N14H mutation might have a greater destabilizing effect on the binding of phosphate to the apoflavodoxin.

The data obtained for the Tyr98 mutants also agreed with this model, although the phosphate effects were only examined in detail for the Y98A mutant. All of the mutants behaved like the wild-type apoprotein, exhibiting both slow and fast kinetic phases in 50 mM sodium phosphate buffer (pH 7.0). The removal of the aromatic side chain at this position (i.e., Y98A or Y98M) resulted in a much slower rate for FMN fluorescence quenching and caused the amplitude of the faster phase to decrease to less than 10% of the total. Neither of these mutants bound riboflavin appreciably in these experiments. The side chain of Tyr98 is coplanar to the isoalloxazine ring of the flavin and likely participates in a strong aromatic interaction with the flavin, especially in the oxidized state (*17*, *25*). This interaction appears to be crucial for the binding of flavins without a 5′-phosphate group. As mentioned previously, at the ionic strength used in the phosphate competition experiments, the Y98A mutant showed only one binding phase and the binding rate was inhibited by phosphate. On the basis of these data, together with the observation that Y98A bound riboflavin very weakly (>0.5 mM), we propose that this mutant is unable to bind via the ring-first mode, due to the loss of the aromatic residue.

The indole ring flanking the *re* face of the isoalloxazine ring (Trp60) also appears to be important for the binding of flavin. As seen in Table 4, the binding of FMN to this mutant was even weaker than for the Y98A mutant. Riboflavin also did not bind to this mutant, again suggesting the important nature of the interactions of the flanking aromatic residues in the binding of flavins without phosphate. Like for the wild-type apoprotein, binding of FMN to W60A occurred in two kinetic phases. However, unlike those for the wild type or any of the other mutants used in this study, both phases of FMN binding to the W60A apoflavodoxin were inhibited by inorganic phosphate. Thus, the removal of the aromatic side chain at this position seemed to initiate a different binding mechanism that either may be hidden by the ring-first phase in the others or may be a direct result of this new mutation. It is important to note that Trp60 makes contacts with both the isoalloxazine ring and the ribityl side chain in the holoprotein complex. It is possible that the FMN binds differently to the W60A mutant as a result. Further data from other studies (*16*) also confirm the importance of this residue in the binding modes of FMN and riboflavin.

Are there other binding mechanisms that could be derived from the fluorescence quenching kinetic results? Several characteristic mechanisms are excluded by the data. A strictly second-order binding process is obviously excluded by the biphasic kinetic pattern and the phosphate dependencies. A single kinetic phase would also be expected if the isoalloxazine ring of the flavin could not bind until the phosphate triggered the opening of its subsite. Another possibility would be two conformations of protein that bind phosphate-first, but quench the fluorescence of the isoalloxazine ring at different rates. Although this fits with the observed concentration dependence data, in that both phases would be dependent on the enzyme concentration, this model is not consistent with the phosphate competition data. Also, it is difficult to rationalize why the two conformations would bind riboflavin at equal rates as would be necessary for accommodation of the monophasic kinetics observed for this flavin. Another plausible mechanism would be the initial binding of the flavin followed by some type of rearrangement or conformational change that further quenches the flavin fluorescence, yielding the final holoprotein complex as suggested by earlier research (*7*, *8*). However, while this binding mechanism does accommodate the biphasic kinetic quenching, the model would also predict that the second phase would be independent of the concentration of enzyme under pseudo-first-order conditions such as those in our experiments. It also cannot explain the phosphate competition data. Thus, the phosphate- and ring-first binding model discussed above seems to fit best all of the data that have been collected.

Is it possible to reconcile this mechanism with structural data? In the holoflavodoxin structure of *D. vulgaris* (*3*), there is a hydrogen bonding network from the phosphate group of the FMN, through Ser58, to the indole nitrogen of the tryptophan residue on the *re* face of the isoalloxazine ring (Trp60). This network provides a direct link from the phosphate in the phosphate-binding subsite to one of the aromatic residues in the ring-binding site. In the accompanying paper (*16*), evidence of physical changes in this tryptophan residue is provided that supports this hypothesis.

Conclusions. The data in this paper show that, in contrast to earlier studies (*11*, *12*), the binding of FMN to the flavodoxin from *D. vulgaris* does not occur as a simple second-order reaction. In the presence of phosphate, two kinetic phases for the fluorescence quenching were observed during the binding of FMN, with the rate for the slower phase decreased and that for the faster phase increased with increasing phosphate concentrations. Only one kinetic phase was observed for the binding of riboflavin, the rate of which increased as the phosphate concentration increased. The data were interpreted by a binding model which, for FMN, includes a ring-first and a phosphate-first binding mode (Scheme 1). Furthermore, all of the phosphate competition and enhancement kinetic data can be fit to a single-site binding isotherm generating an apparent K_d for inorganic phosphate and apoflavodoxin of 45 ± 9 mM. Thus, in the proposed binding mechanism model, phosphate binding, whether from the cofactor itself or by inorganic phosphate, causes a conformational change that promotes the ring binding mode. Because of the absence of the 5′-phosphate group, riboflavin binding can only proceed via the ring-first mode and binding is very weak when there is no free phosphate present. More direct physical evidence for a phosphate-dependent conformational change affecting the ring-binding subsite has also been obtained (*16*). Finally, it is possible that other flavodoxins bind FMN through a different mechanism(s). Most notably, as was the case with the W60A mutant of *D. vulgaris*, there may be differences in the binding mechanisms of flavodoxins that have two aromatic residues flanking the isoalloxazine ring compared to those that have only one.

REFERENCES

1. Mayhew, S. G., and Tollin, G. (1992) in *Chemistry and Biochemistry of Flavoenzymes* (Muller, F., Ed.) pp 389−426, CRC Press, Boca Raton, FL.
2. Ludwig, M. L., and Luschinsky, C. L. (1992) in *Chemistry and Biochemistry of Flavoenzymes* (Muller, F., Ed.) pp 427−466, CRC Press, Boca Raton, FL.
3. Watenpaugh, K. D., Sieker, L. C., and Jensen, L. H. (1973) The binding of riboflavin-5′-phosphate in a flavoprotein: flavodoxin at 2.0-Angstrom resolution, *Proc. Natl. Acad. Sci. U.S.A. 70*, 3857−3860.
4. Hinkson, J. W. (1968) *Azotobacter* free-radical flavoprotein. Preparation and properties of the apoprotein, *Biochemistry 7*, 2666−2672.
5. Mayhew, S. G. (1971) Studies on flavin binding in flavodoxins, *Biochim. Biophys. Acta 235*, 289−302.
6. Edmondson, D. E., and Tollin, G. (1971) Chemical and physical characterization of the Shethna flavoprotein and apoprotein and kinetics and thermodynamics of flavin analog binding to the apoprotein, *Biochemistry 10*, 124−132.
7. D'Anna, J. A., and Tollin, G. (1972) Studies of flavin-protein interaction in flavoproteins using protein fluorescence and circular dichroism, *Biochemistry 11*, 1073−1080.
8. Barman, B. G., and Tollin, G. (1972) Flavine-protein interactions in flavoenzymes. Temperature-jump and stopped-flow studies of flavine analog binding to the apoprotein of *Azotobacter* flavodoxin, *Biochemistry 11*, 4746−4754.
9. Carlson, R., and Langerman, N. (1984) The thermodynamics of flavin binding to the apoflavodoxin from *Azotobacter vinelandii*, *Arch. Biochem. Biophys. 229*, 440−447.
10. Leenders, R., Van Hoek, A., Van Iersel, M., Veeger, C., and Visser, A. J. W. G. (1993) Flavin dynamics in oxidized *Clostridium beijerinckii* flavodoxin as assessed by time-resolved polarized fluorescence, *Eur. J. Biochem. 218*, 977−984.
11. Dubourdieu, M., MacKnight, M. L., and Tollin, G. (1974) Temperature-jump studies of *Desulfovibrio vulgaris* flavodoxin: kinetics of FMN binding and of reduction of semiquinone by methyl viologen, *Biochem. Biophys. Res. Commun. 60*, 649−655.
12. Pueyo, J. J., Curley, G. P., and Mayhew, S. G. (1996) Kinetics and thermodynamics of the binding of riboflavin, riboflavin 5′-phosphate and riboflavin 3′,5′-bisphosphate by apoflavodoxins, *Biochem. J. 313*, 855−861.
13. Watenpaugh, K. D., Sieker, L. C., Jensen, L. H., Legall, J., and Dubourdieu, M. (1972) Structure of the oxidized form of a flavodoxin at 2.5-Angstrom resolution: resolution of the phase ambiguity by anomalous scattering, *Proc. Natl. Acad. Sci. U.S.A. 69*, 3185−3188.
14. Genzor, C. G., Perales-Alcon, A., Sancho, J., and Romero, A. (1996) Closure of a tyrosine/tryptophan aromatic gate leads to a compact fold in apoflavodoxin, *Nat. Struct. Biol. 3*, 329−332.
15. Steensma, E., and van Mierlo, C. P. M. (1998) Structural Characterisation of Apoflavodoxin shows that the Location of the Stable Nucleus Differs Among Proteins with a Flavodoxin-like Topology, *J. Mol. Biol. 282*, 653−666.
16. Murray, T. A., Foster, M. P., and Swenson, R. P. (2003) Mechanism of Flavin Mononucleotide Cofactor Binding to the *Desulfovibrio vulgaris* Flavodoxin. 2. Evidence for Cooperative Conformational Changes Involving Tryptophan 60 in the Interaction between the Phosphate- and Ring-Binding Subsites, *Biochemistry 42*, 2317.
17. Swenson, R. P., and Krey, G. D. (1994) Site-directed mutagenesis of tyrosine-98 in the flavodoxin from *Desulfovibrio vulgaris* (Hildenborough): regulation of oxidation−reduction properties of the bound FMN cofactor by aromatic, solvent, and electrostatic interactions, *Biochemistry 33*, 8505−8514.

18. Zhou, Z., and Swenson, R. P. (1996) Evaluation of the electrostatic effect of the 5′-phosphate of the flavin mononucleotide cofactor on the oxidation−reduction potentials of the flavodoxin from *Desulfovibrio vulgaris* (Hildenborough), *Biochemistry 35*, 12443−12454.
19. Kunkel, T. A. (1985) Rapid and efficient site-specific mutagenesis without phenotypic selection, *Proc. Natl. Acad. Sci. U.S.A. 82*, 488−492.
20. Wassink, J. H., and Mayhew, S. G. (1975) Fluorescence titration with apoflavodoxin: a sensitive assay for riboflavin 5′-phosphate and flavin adenine dinucleotide in mixtures, *Anal. Biochem. 68*, 609−616.
21. Pace, C. N., Vajdos, F., Fee, L., Grimsley, G., and Gray, T. (1995) How to measure and predict the molar absorption coefficient of a protein, *Protein Sci. 4*, 2411−2423.
22. Druhan, L. J., and Swenson, R. P. (1998) Role of methionine 56 in the control of the oxidation−reduction potentials of the *Clostridium beijerinckii* flavodoxin: effects of substitutions by aliphatic amino acids and evidence for a role of sulfur-flavin interactions, *Biochemistry 37*, 9668−9678.
23. Whitby, L. G. (1953) *Biochem. J. 54*, 437−442.
24. Curley, G. P., Carr, M. C., Mayhew, S. G., and Voordouw, G. (1991) Redox and flavin-binding properties of recombinant flavodoxin from *Desulfovibrio vulgaris* (Hildenborough), *Eur. J. Biochem. 202*, 1091−1100.
25. Zhou, Z., and Swenson, R. P. (1996) The cumulative electrostatic effect of aromatic stacking interactions and the negative electrostatic environment of the flavin mononucleotide binding site is a major determinant of the reduction potential for the flavodoxin from *Desulfovibrio vulgaris* [Hildenborough], *Biochemistry 35*, 15980−15988.
26. Walsh, M. A., McCarthy, A., O'Farrell, P. A., McArdle, P., Cunningham, P. D., Mayhew, S. G., and Higgins, T. M. (1998) X-ray crystal structure of the *Desulfovibrio vulgaris* (Hildenborough) apoflavodoxin-riboflavin complex, *Eur. J. Biochem. 258*, 362−371.
27. Gast, R., Valk, B. E., Muller, F., Mayhew, S. G., and Veeger, C. (1976) Studies on the binding of FMN by apoflavodoxin from *Peptostreptococcus elsdenii*, pH and NaCl concentration dependence, *Biochim. Biophys. Acta 446*, 463−471.
28. Lostao, A., El Harrous, M., Daoudi, F., Romero, A., Parody-Morreale, A., and Sancho, J. (2000) Dissecting the energetics of the apoflavodoxin-FMN complex, *J. Biol. Chem. 275*, 9518−9526.

BI026967S